

# Porphyromonas gingivalis lipopolysaccharide regulates cell proliferation, apoptosis, autophagy in esophageal squamous cell carcinoma via TLR4/MYD88/JNK pathway

Chi Lu,<sup>1,†</sup> Zhiguo Chen,<sup>2,†</sup> Hongda Lu,<sup>1,\*</sup> and Ke Zhao<sup>2,\*</sup>

<sup>1</sup>Department of Oncology and <sup>2</sup>Department of Thoracic Surgery, The Central Hospital of Wuhan, Tongji Medical College, Huazhong University of Science and Technology, Wuhan 430014, China

(Received 30 November, 2022; Accepted 3 April, 2023; Released online in J-STAGE as advance publication 23 November, 2023)

The study aimed to explore the impact and potential mechanism of *Porphyromonas gingivalis* lipopolysaccharide (LPS-PG) on esophageal squamous cell carcinoma (ESCC) cell behavior. ESCC cells from the Shanghai Cell Bank were used, and TLR4, MYD88, and JNK interference vectors were constructed using adenovirus. The cells were divided into six groups: Control, Model, Model + radiotherapy + LPS-PG, Model + radiotherapy + 3-MA, Model + radiotherapy + LPS-PG + 3-MA, and Model + radiotherapy. Various radiation doses were applied to determine the optimal dose, and a radioresistant ESCC cell model was established and verified. CCK8 assay measured cell proliferation, flow cytometry and Hoechst 33258 assay assessed apoptosis, and acridine orange fluorescence staining tested autophagy. Western blot analyzed the expression of LC3II, ATG7, P62, and p-ULK1. Initially, CCK8 and acridine orange fluorescence staining identified optimal LPS-PG intervention conditions. Results revealed that 10 ng/ml LPS-PG for 12 h was optimal. LPS-PG increased autophagy activity, while 3-MA decreased it. LPS-PG + 3-MA group exhibited reduced autophagy. LPS-PG promoted proliferation and autophagy, inhibiting apoptosis in radioresistant ESCCs. LPS-PG regulated TLR4/MYD88/JNK pathway, enhancing ESCC autophagy, proliferation, and radioresistance. In conclusion, LPS-PG, through the TLR4/MYD88/JNK pathway, promotes ESCC proliferation, inhibits apoptosis, and enhances radioresistance by inducing autophagy.

**Key Words:** porphyromonas gingivalis lipopolysaccharide, autophagy, esophageal squamous cell carcinoma, TLR4/MYD88/JNK

Esophageal cancer (EC) is the second most common tumor of digestive tract in the world. About 300,000 people die of EC every year in the world, which is one of the main tumor types threatening human health.<sup>(1,2)</sup> Up to now, the incidence of EC in China ranks the first in the world, and the mortality rate ranks the fourth. Therefore, the prevention and treatment of EC is one of the major public health problems that need to be solved urgently in China.<sup>(3,4)</sup> At present, endoscopic treatment is the main treatment for EC in the early stage,<sup>(5)</sup> and surgery is the first choice for the treatment of EC in the middle and late stage. However, as the surgical treatment of EC requires clear indications, the patients who can be treated with radical surgery only account for 1/4 of all EC patients.<sup>(6,7)</sup> Thus, radiotherapy is one of the main, effective and safe treatment methods for middle-advanced EC at present. It has a wide indication and can effectively improve the symptoms of patients. However, due to adverse reactions such as drug tolerance, its efficacy is seriously affected, and even leads to

radiotherapy failure. Therefore, it is of great clinical significance to find the potential mechanism of radiotherapy tolerance in the treatment of EC.

Studies have found that radiation can induce the increase of autophagy activity and lead to radiation resistance in liver cancer cells, breast cancer cells and brain glioma cells. Autophagy plays a crucial role in adapting cells to multiple stresses, recycling excess or damaged cellular material, quality control of organelles, removal of protein aggregates, and destruction of intracellular pathogens.<sup>(8)</sup> Clinicopathological studies have shown that autophagy activity is elevated in patients with NSCLC and is associated with worsening health status.<sup>(9)</sup> Autophagy activation is a tumor survival strategy, through which it can resist radiation-mediated cell damage. Inhibition of autophagy activation leads to radiosensitivity of HNSCC cells.<sup>(10)</sup> Autophagy plays a dual role in the response of cancer cells to ionizing radiation. On the one hand, autophagy inhibition can increase radiation-induced tumor cell death and inhibit tumor growth, while reducing the survival rate of cell clonogenesis. On the other hand, defects in autophagy can reduce the efficacy of radiotherapy.<sup>(11)</sup> Liu *et al.*<sup>(12)</sup> demonstrated that autophagy flux was accelerated after 5 consecutive 2 Gy fractions were applied in A549 lung cancer cells. In previous studies, our research team found that autophagy activation can promote the survival of esophageal squamous cell carcinoma cells. The autophagy inhibitor chloroquine combined with radiotherapy can effectively reduce the size of esophageal squamous cell carcinoma (ESCC), increase the apoptosis of ESCC.<sup>(13,14)</sup> Studies have found that LPS-PG also plays an important role in ESCC,<sup>(1-3)</sup> and LPS-PG can affect the proliferation, migration and autophagy of ESCC,<sup>(4-6)</sup> but there are few studies on the effect and mechanism of LPS-PG on the production of radiation resistance to ESCC. On this basis, we conducted preliminary experiments, suggesting that *porphyromonas gingivalis* can induce autophagy activation through TLR4/MYD88/JNK pathway and promote the radioresistance of ESCC.

Thus, the aim of this study was to evaluate the effect of *porphyromonas gingivalis* lipopolysaccharide (LPS-PG) on ESCCs proliferation, apoptosis and autophagy, explore the mechanism by which LPS-PG contributes to radioresistance in ESCCs by inducing autophagy activation, and identify the important role of TLR4/MyD88/JNK pathway.

<sup>†</sup>They are contributed equally.

\*To whom correspondence should be addressed.

E-mail: phlonda66@hotmail.com (HL); kzhaol23@163.com (KZ)

## Materials and Methods

**Cell culture.** KYSE-150 cells were obtained from the Shanghai Cell Bank, Chinese Academy of Sciences. The cells were cultured in RPMI-1640 (SH30809.01B; Hyclone, Logan, UT) supplemented with 10% fetal bovine serum (FBS, 10270-106; Gibco, Grand Island, NE), and cultured in a 37°C constant temperature incubator (5% CO<sub>2</sub>). The medium was replaced every 24 h, and the cells were subcultured or cryopreserved when the confluence reached 80–90%.

**Construction of acquired radioresistant esophageal squamous cell carcinoma cell model.** KYSE-150 cells in exponential growth stage were irradiated with 6MVX-ray using a linear accelerator (irradiation field 10 cm × 10 cm, source-target distance 100 cm, dose rate 200 cGy/min), and the first irradiation was 100 cGy. After that, the cells were returned to the incubator and cultured. When the cells grew to 90%, they were subcultured by trypsin digestion and irradiated with 100 cGy. The above process was repeated, and each dose of 100, 200, and 400 cGy was irradiated 3 times, with a total of 2,100 cGy.

KYSE-150 cells were intervention with LPS-PG and autophagy inhibitor (3-MA, 6 mM) for 12 h, and respectively divided into six groups: Control, Model (acquired radioresistant ESCC), Model + radiotherapy + LPS-PG (trlr-pglps; InvivoGen, Toulouse, France), Model + radiotherapy + 3-MA, Model + radiotherapy + LPS-PG + 3-MA, and Model + radiotherapy group.

**Cell transfection.** The full-length cDNA of TLR4 (GI: 194068428), MYD88 (GI: 1764714898), and JNK (GI: 1890270517) were obtained from the NCBI database. Cells were transfected with sh-TLR4, sh-MYD88 or sh-JNK using Lipofectamine 2000 reagent according to the manufacturer's instructions. 2 h before transfection, 2 µg of recombinant adenovirus vector plasmid and 4 µg of skeleton plasmid pHBA-BHG were transfected. Diluted with 300 µl of DMEM (31985-062; Hyclone) medium and left at room temperature for 5 min, then dilute 15 µl Lipofectamine<sup>®</sup> RNAiMAX (11668-027; Invitrogen, Carlsbad, CA) in 300 µl DMEM, mixed and incubated at 4°C for 5 min. Then place the cell culture plate in a 37°C, 5% CO<sub>2</sub> incubator for 6 h. Then, the phenomenon of cell toxicity was observed every day. When most of the cell lesions fell off from the bottom, the cells were collected and expanded, purified and dialyzed, and then the cells were separated and stored at -80°C refrigerator.

**Cell counting kit-8.** 3 × 10<sup>3</sup> cells were seeded in a 96-well plate using RPMI 1640 medium containing 10% FBS and treated for 12, 24, 48, and 72 h. To evaluate cell proliferation, 10 µl of cell counting kit-8 (CCK-8) solution was added to each well and the cells were cultured at 37°C for 4 h. The optical density (OD) was measured using a microplate reader (Multiskan FC; Thermo, Waltham, MA) at 450 nm.

**Clone formation assay.** 2 × 10<sup>3</sup> cells were seeded in a 6-well plate using RPMI 1640 medium containing 10% FBS and incubated in an incubator with 5% CO<sub>2</sub> at 37°C. When macroscopic cloning appeared in the 6-well plate, 0.25% trypsin (T1350; solarbio, Beijing, China) was added to stop the culture. After washing twice with PBS, 2 ml of 4% paraformaldehyde was added and fixed at 4°C for 15 min. Then 1 ml of Reiss-Giemsa composite dye solution (G1020; solarbio) was added for 20 min, and the plates were observed under an inverted microscope (DMIL LED; Leica, Heidelberg, Germany).

**Hoechst 33258 assay.** Cells were immobilized with 4% paraformaldehyde for 20 min and washed twice with PBS in 12-well plates. 1 ml of Hoechst 33258 dye solution was added and the cells were stained at 4°C for 5 min. Cell morphology and apoptosis were observed by fluorescence microscopy (DMIL LED).

**Flow cytometry.** Cells in each group were cultured for 12 h and then harvested, added in 1 ml pre-cooled PBS, and centrifuge

**Table 1.** Primer sequences

Primer	Sequence (5'-3')
TLR4-F	AGGATGAGGACTGGGTAAGGA
TLR4-R	TGCTGGGACACCACAACAAT
MYD88-F	GGATGGTGGTGGTTGTCTC
MYD88-R	CTTCATTGCCTTGTACTTGATG
JNK-F	TGGGCTACAAGGAAAACG
JNK-R	TGGGAAAAGGACATCAGG
GAPDH-F	GGGAACTGTGGCGTGAT
GAPDH-R	GAGTGGGTGTCGCTGTGA

at 1,000 × g, cell apoptosis analyzed using flow cytometry according to the manufacturer's instructions (556547; BD) and the data were analyzed by flow cytometry (Beckman Coulter, Brea, CA).

**Acridine orange fluorescence staining.** Cells were immobilized with 4% paraformaldehyde for 20 min and washed twice with PBS. AO Stain Buffer and AO Stain (DA0037; Regan, Beijing, China) were mixed at a ratio of 19:1, and cells were cultured in it for 15 min at room temperature. Then wash with PBS twice, 1 min each time, and place it under an inverted microscope for observation (DMIL LED).

**Quantitative reverse transcription polymerase chain reaction.** Whole RNA of the cell samples were extracted using Trizol reagent according to the manufacturer's procedures, cDNA was synthesized using reverse transcriptase kit (TAKARA, Osaka, Japan). Quantitative reverse transcription polymerase chain reaction (qRT-PCR) was performed in Real-Time System (BIO-RAD, Hercules, CA) by using YBR Green PCR Kit (KM4101; KAPA Biosystems, Santiago, CA). Each qPCR reaction was performed in duplicate. The results analysis by 2<sup>-ΔΔCt</sup> method. The primers were designed and configured by Nanjing Kingsy Biotechnology Co., Ltd., Nanjing, China (Table 1).

**Western blot analysis.** The protein from cells was extracted and the concentration was measured by BCA protein assay kit (Beyotime, Shanghai, China). Total protein was separated in 12% SDS-PAGE and transferred to PVDF membranes. The membranes were blocked with a buffer containing 5% non-fat milk in PBS with 0.05% Tween-20 for 2 h and incubated with primary antibody used included anti-p62 antibody (1:1,000, PAB35470; Bioswamp, Wuhan, China), anti-LC3II antibody (1:1,000, PAB34124; Bioswamp), anti-p-ULK1 antibody (1:1,000, ab179458; abcam), anti-ULK1 antibody (1:1,000, PAB35960; Bioswamp), anti-ATG7 antibody (1:1,000, PAB30187; Bioswamp), anti-TLR4 antibody (1:1,000, PAB33926; Bioswamp), anti-MYD88 antibody (1:1,000, PAB36760; Bioswamp), anti-JNK antibody (1:1,000, PAB30101; Bioswamp), and anti-GAPDH antibody (1:1,000, PAB36269; Bioswamp). After three washes with PBS/Tween 20, the membranes were incubated with horseradish peroxidase-conjugated secondary goat anti-rabbit IgG (1:20,000, SAB43714; Bioswamp) for 2 h at room temperature. Protein bands were visualized by enhanced chemiluminescence color detection (Tanon-5200; TANON, Shanghai, China) and analyzed using TANON GIS software.

**Data analysis and statistics.** All data are presented as mean ± SD. The SPSS 19.0 software was used for statistical analyses and the GraphPad prism 5.0 was used to draw the figures. The data were evaluated for statistical significance using the one-way ANOVA test. Statistical significance was established at *p* < 0.05.

## Results

**Effect of LPS-PG on ESCC cell autophagy.** Firstly, CCK8 and acridine orange staining were used to detect the autophagy and proliferation ability of ESCC cells, respectively. According

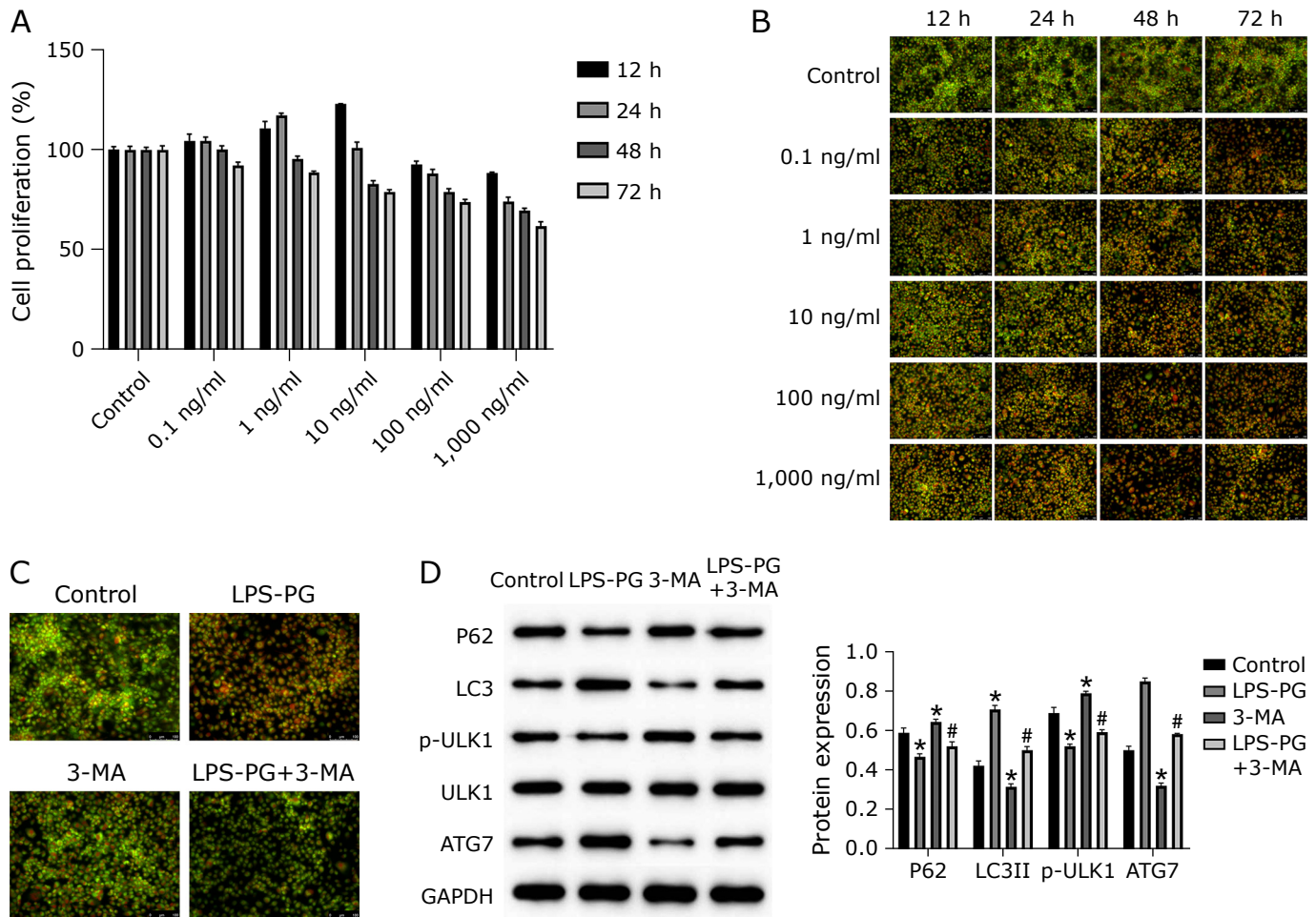


**Fig. 1.** Effect of LPS-PG on ESCC cell autophagy. (A) CCK8 was used to detect the esophageal squamous cell carcinoma cell proliferation at 12, 24, 48, and 72 h. (B, C) Autophagy was detected by acridine orange fluorescence staining at different time points (scale bar = 100  $\mu$ m). (D) Western blot analysis of LC3II, ATG7, p62, and p-ULK1 expression. \* $p < 0.05$  vs Control; # $p < 0.05$  vs LPS-PG.  $n = 3$ .

to the activation degree and proliferation ability of autophagy, the optimal intervention concentration and time of LPS-PG were screened. As shown in Fig. 1A and B, the optimal intervention concentration of LPS-PG was 10 ng/ml and the action time was 12 h. The optimal concentration and time of LPS-PG selected in the above experiments were then used for subsequent experiments, and the results were shown in Fig. 1C, compared with the control group, the autophagy activity of the cells in the LPS-PG group was significantly increased, while the autophagy activity of the cells in the 3-MA group was decreased. Compared with the LPS-PG group, autophagy was decreased in the LPS-PG + 3-MA group. Autophagy related proteins p62, LC3II, p-ULK1 and ATG7 were tested by Western blot. Compared with the control group, the expression of LC3II and ATG7 in LPS-PG group was significantly increased ( $p < 0.05$ ), while the expression of p62 and p-ULK1 was significantly decreased ( $p < 0.05$ ). In 3-MA group, the expression of LC3II and ATG7 decreased significantly ( $p < 0.05$ ), while the expression of p62 and p-ULK1 increased significantly ( $p < 0.05$ ). Compared with the LPS-PG group, the expressions of LC3II and ATG7 in the LPS-PG + 3-MA group were decreased ( $p < 0.05$ ), and the expressions of p62 and P-ULK1 were increased ( $p < 0.05$ ) (Fig. 1D), suggesting that LPS-PG could promote autophagy in ESCC cells.

**Effect of LPS-PG on cell proliferation and autophagy of acquired radioresistant ESCCs.** In order to determine the optimal radiation dose, we used different doses of radiation

to intervene the cells, and then detected the cell activity and apoptosis through CCK8 and flow cytometry. The results showed that the optimal radiation dose was 2 Gy (Fig. 2A and B). Plate cloning experiment showed that the clone number of cells in the 2 Gy group was decreased compared with that in the control group ( $p < 0.05$ ) (Fig. 2C), indicating that the acquired radioresistant ESCC cell model was successfully constructed. Compared with the control group, the cell proliferation of the Model group was decreased ( $p < 0.05$ ). Compared with Model + radiotherapy group, the cell proliferation of Model + radiotherapy + LPS-PG group was increased ( $p < 0.05$ ), while that of Model + radiotherapy + 3-MA group was decreased ( $p < 0.05$ ). Compared with Model + radiotherapy + LPS-PG group, the cell proliferation of Model + radiotherapy + LPS-PG + 3-MA group was decreased ( $p < 0.05$ ) (Fig. 2D). We further tested the autophagy associated proteins and the results showed that compared with the control group, the expressions of P62 and p-ULK1 in the Model group were increased ( $p < 0.05$ ), while the expressions of LC3II and ATG7 were decreased ( $p < 0.05$ ). Compared with Model + radiotherapy group, The expressions of LC3II and ATG7 in Model + radiotherapy + LPS-PG group were significantly increased ( $p < 0.05$ ), while the contents of P62 and p-ULK1 in Model + radiotherapy + 3-MA group were significantly increased ( $p < 0.05$ ). Compared with Model + radiotherapy + LPS-PG group, the levels of P62 and p-ULK1 in Model + radiotherapy + LPS-PG + 3-MA group were increased ( $p < 0.05$ ), while the levels of

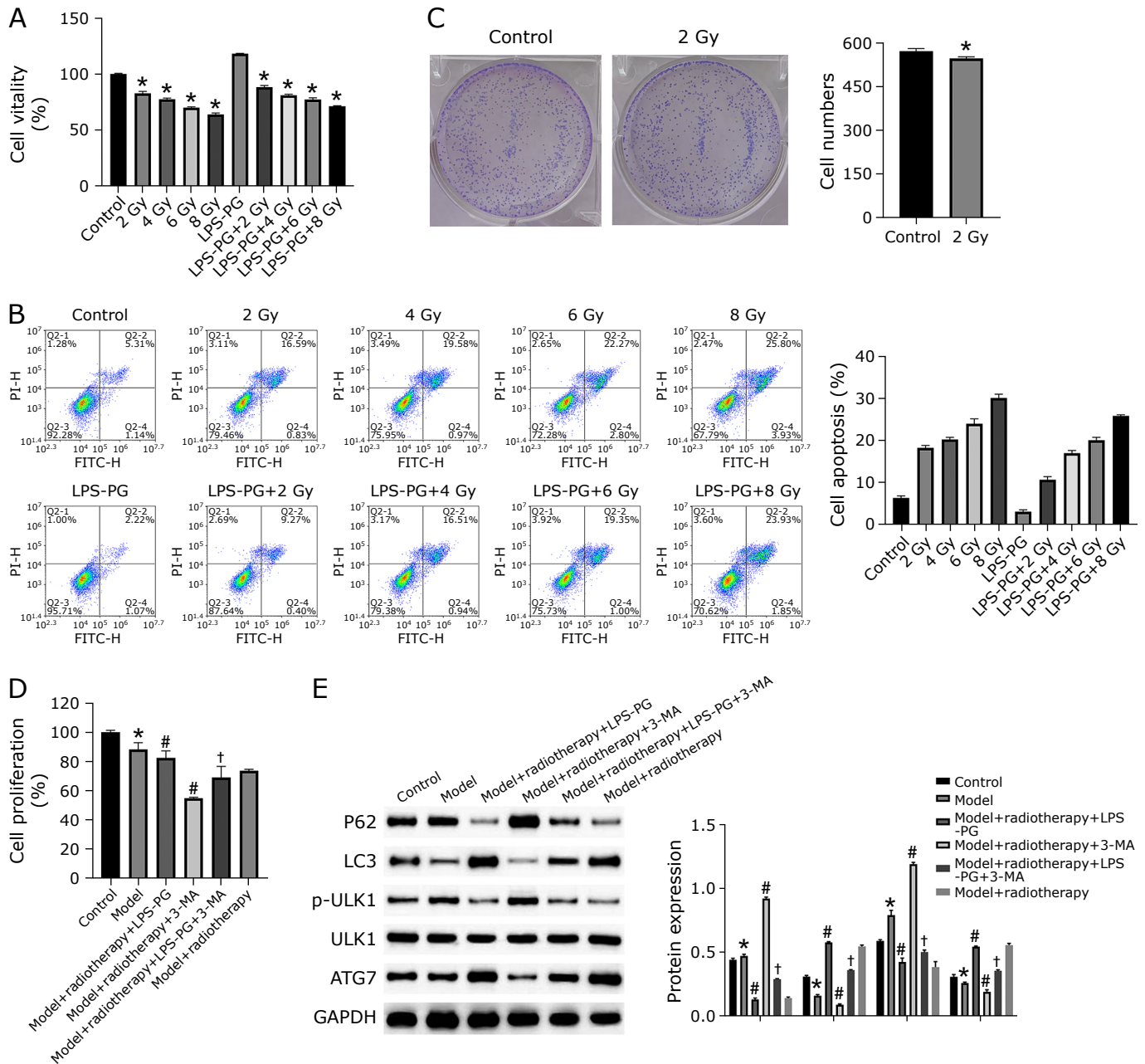


**Fig. 2.** Effect of LPS-PG on cell proliferation and autophagy of acquired radioresistant ESCCs. (A) CCK8 was used to detect the cell vitality at different radiation dose. (B) Cell apoptosis were detected by flow cytometry at 2, 4, 6, and 8 Gy. (C) Clone formation assay was used to measure the number of clone cells. (D) CCK8 was used to measure cell proliferation. (E) LC3II, ATG7, p62, and p-ULK1 expression was test by Western blot. \* $p < 0.05$  vs Control; # $p < 0.05$  vs Model + radiotherapy; † $p < 0.05$  vs Model + radiotherapy + LPS-PG,  $n = 3$ .

LC3II and ATG7 were decreased ( $p < 0.05$ ) (Fig. 2E). These results suggest that LPS-PG can promote the proliferation and autophagy of acquired radioresistant ESCCs, and inhibit their apoptosis.

**Effect of LPS-PG on TLR4/MYD88/JNK pathway.** We first constructed the interference recombinant adenovirus of TLR4, MYD88, and JNK respectively, and then used PCR to verify the transfection efficiency. As shown in Fig. 3A, compared with the control group, the expression of target protein in each interference group was significantly decreased ( $p < 0.05$ ), indicating successful transfection. Compared with the control group, the expressions of TLR4, MYD88, and JNK in 3-MA group were decreased ( $p < 0.05$ ). Compared with 3-MA group, the contents of TLR4, MYD88, and JNK in LPS-PG + 3-MA group had no

significant differences ( $p > 0.05$ ) (Fig. 3B). Acridine orange staining was used to detect whether LPS-PG played a role in ESCC cell autophagy by regulating TLR4/MYD88/JNK pathway. The results showed that under the precondition of inhibiting TLR4, MYD88, and JNK activities, autophagy increased in the LPS-PG group and LPS-PG + 3-MA group compared with the control group (Fig. 3C). We further detected the expression changes of LC3II, ATG7, p62, and p-ULK1 in each group, and the results were shown in Fig. 3D. Compared with the control group, the expression levels of LC3II and ATG7 in the LPS group and LPS-PG + 3-MA group were increased ( $p < 0.05$ ), while the contents of P62 and p-ULK1 were decreased ( $p < 0.05$ ), and the autophagy-related proteins in the 3-MA group showed an opposite trend, suggesting that LPS-PG could regulate

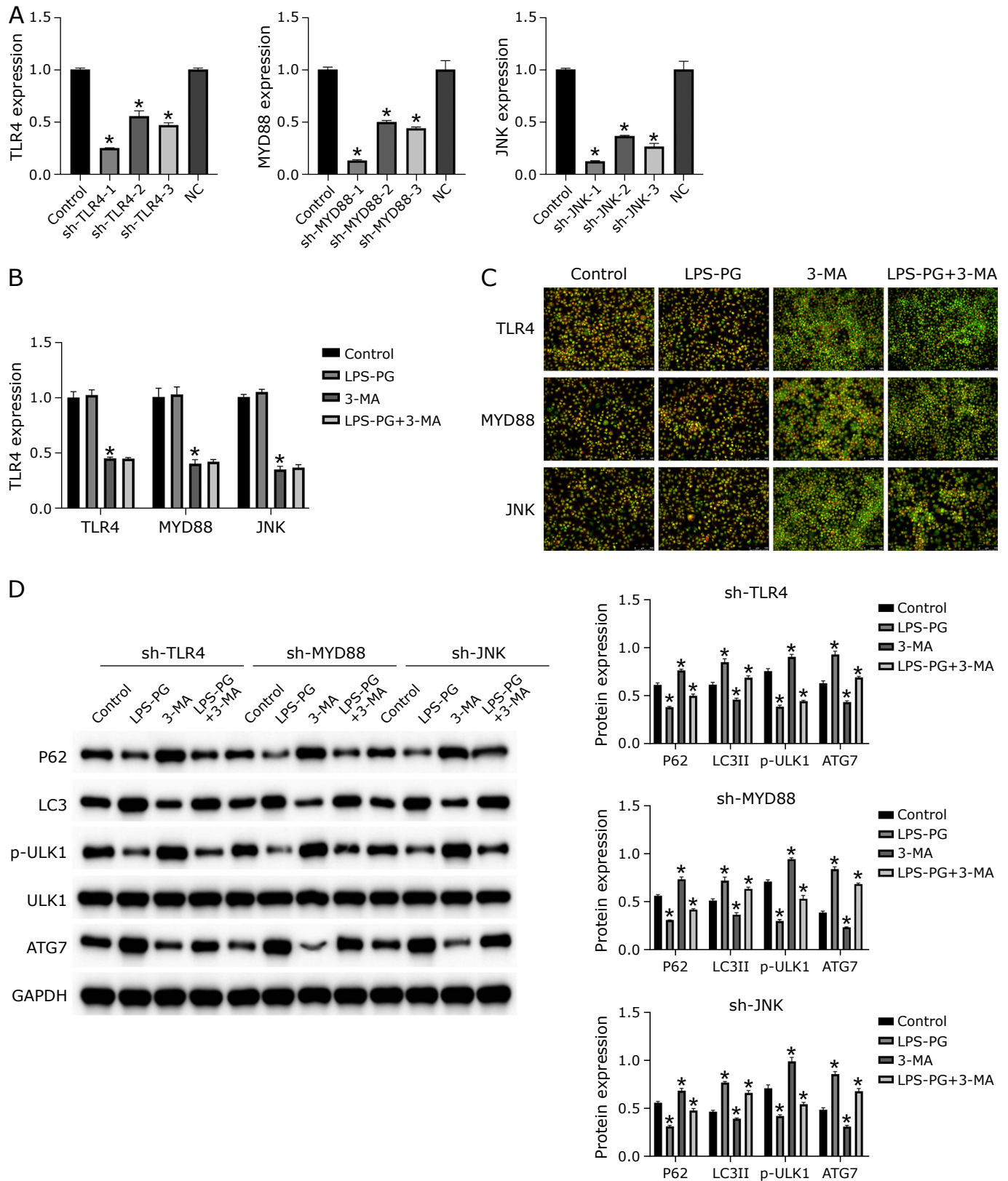


**Fig. 3.** Effect of LPS-PG on TLR4/MYD88/JNK pathway of ESCCs. (A, B) TLR4, MYD88, and JNK mRNA were observed by RT-PCR. (C) Acridine orange fluorescence staining was used to test cell autophagy (scale bar = 100  $\mu$ m). (D) Under the premise of sh-TLR4, sh-MYD88, and sh-JNK intervention respectively, Western blot analysis of LC3II, ATG7, p62, and p-ULK1 expression. \* $p$ <0.05 vs Control,  $n$  = 3.

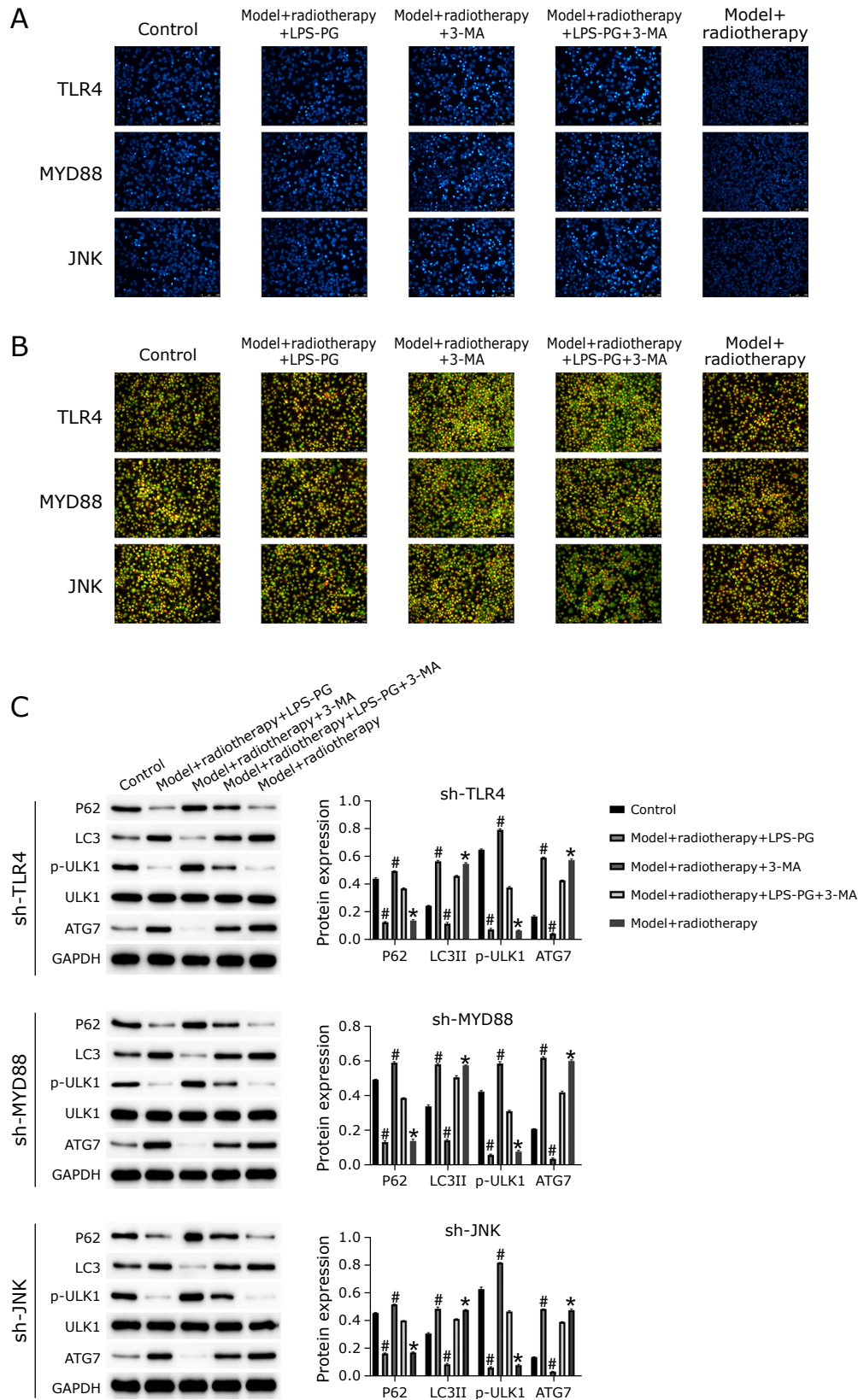


**Fig. 4.** Effect of LPS-PG on TLR4/MYD88/JNK pathway of acquired radioresistant ESCCs. (A) Under the premise of sh-TLR4, sh-MYD88, and sh-JNK intervention respectively, Hoechst 33258 method was used to detect the apoptosis of cells in each group (scale bar = 100  $\mu$ m). (B) Acridine orange fluorescence staining was used to test cell autophagy (scale bar = 100  $\mu$ m). (C) LC3II, ATG7, p62, and p-ULK1 expression was detected by Western blot after intervening separately with sh-TLR4, sh-MYD88, and sh-JNK. \* $p < 0.05$  vs Control; # $p < 0.05$  vs Model + radiotherapy,  $n = 3$ .

the autophagy activation of ESCC cells through TLR4/MYD88/JNK pathway. Thus, we wondered whether LPS-PG could also regulate autophagy in acquired radioresistant ESCCs through the TLR4/MYD88/JNK pathway. Acridine orange staining, Hoechst 33258 staining and WB staining were used to observe the changes of cell characteristics. Compared with the control group, cell apoptosis in the Model + radiology group was reduced. Compared with Model + radiology group, apoptosis in Model + radiology + LPS-PG group decreased, while the cell apoptosis in Model + radiology + 3-MA group increased (Fig. 4A). Acridine orange staining and WB were used to detect autophagy. The results are shown in Fig. 4B and C. Compared with the control group, autophagy in Model + radiotherapy group was increased, LC3II and ATG7 contents were increased ( $p < 0.05$ ), and the expression of P62 and P-ULK1 was decreased ( $p < 0.05$ ). Compared with Model + radiotherapy group, cell autophagy, LC3II and ATG7 levels were increased in LPS-PG + Model + radiotherapy group ( $p < 0.05$ ). Autophagy activity in 3-MA + Model + radiotherapy group was decreased, and the P62 and p-ULK1 expression were significantly increased ( $p < 0.05$ ).

## Discussion

EC has a high morbidity and mortality rate, with a 5-year survival rate of less than 20%. ESCC and esophageal adenocarcinoma are more common in histopathology.<sup>(15)</sup> ESCC is caused by the malignant differentiation of esophageal squamous epithelial cells, and its main characteristics are the overexpression of EGFR and cyclin D1 and the mutation of P53.<sup>(16)</sup> The poor prognosis of EC patients is mainly related to late diagnosis, frequent metastasis and drug resistance.<sup>(17)</sup> The local recurrence and poor local control rate of esophageal cancer are one of the main reasons for the failure of radiotherapy for esophageal cancer, and there are individual differences in the response of esophageal cancer to radiotherapy, which are related to the generation of radiation resistance. Therefore, the study of tumor radioresistance has always been a hot topic in tumor radiotherapy.

Autophagy is a process in which self-damaged organelles and proteins are separated in autophagic vesicles (AVs) and transported to lysosomes for catabolism.<sup>(18)</sup> AVs fuse with lysosomes to degrade autophagy products, produce energy and serve as substrates for biosynthesis, which play an important role in cell proliferation, differentiation and senescence. Autophagy has been proved to be closely related to a variety of diseases, and its role in tumors is very complex. Autophagy plays a tumor suppressor role in early tumors, while in advanced tumors or anti-tumor treatment, stress factors such as nutritional deficiency, DNA damage and cytotoxic effects can induce autophagy and promote the malignant progression of tumors.<sup>(19)</sup> Chen *et al.*<sup>(20)</sup> found that autophagy could be induced in the same cell line by very low doses of radiation, while it was resistant to subsequent higher doses of radiation. Autophagy is known to be essential for cellular homeostasis because it involves the degradation of misfolded proteins and the removal of dysfunctional organelles such as mitochondrial lysosomal degradation machinery. Thus, as a stress response pathway, autophagy can confer protective effects against external stress to promote cell survival.<sup>(21)</sup> Numerous evidences show that autophagy is up-regulated by chemotherapy, radiotherapy or hypoxia.<sup>(22)</sup> Cell populations with high autophagy activity (such as hypoxic cells and stem cells) persist in tumors, which may be one of the reasons for radioresistance of tumors. As a sorting protein of AVs, LC3 is involved in the formation of autophagosomes. The expression level of LC3 in EC is helpful to monitor the disease progression of patients. EC patients with high LC3 expression have an increased rate of adverse reactions and a decreased overall survival rate after adjuvant chemoradiotherapy,<sup>(23)</sup> which may be caused by the accumulation of undegraded autophagosomes caused by the activation of

autophagy pathway or autophagy injury. Compared with ESCC patients with low expression of LC3 and p53, patients with high expression of LC3 and p53 have lower 5-year survival rate.<sup>(24)</sup> LC3 positive signal was mainly stained in cytoplasm, and its punctate structure aggregation was also positively correlated with ki-67.<sup>(25)</sup> P62 is a ubiquitin binding protein involved in cell signaling, oxidative stress and autophagy degradation. P62 promotes the turnover of polyubiquitinated protein aggregates and is a target for the regulation of lysosomal degradation pathways. P62 level in EC tumor tissues is higher than that in normal esophageal mucosa, and the mortality of EC patients with low P62 expression is high.<sup>(26)</sup> Therefore, in this study, we first observed the effect of LPS-PG on autophagy of ESCC cells, and the results showed that after LPS-PG intervention, the autophagy activity of ESCC cells significantly increased, the expression of LC3II and ATG7 increased, and the levels of p62 and p-ULK1 decreased. We further examined the effect of LPS-PG on ESCC cells which had become radiation-resistant. The results showed that compared with the control group, the cells treated with LPS-PG had increased autophagy activity, increased cell proliferation and decreased apoptosis. Compared with the LPS-PG group, the above situation was reversed after the simultaneous administration of LPS-PG and 3-MA.

Inflammation is a defense response of living tissues to the damage caused by external factors. It is a complex protective measure used by the body's own immune system to remove harmful stimuli and promote tissue repair. The initiation of inflammation in the body is mainly through pattern recognition receptors (PRRs) to recognize relevant molecular patterns, and then activate the defense mechanism and release inflammatory mediators. Toll-like receptor (TLR) is one of the important inflammatory recognition receptors, which is a very important molecular receptor in the process of pathogen related risk factors. TLR4, as a pattern recognition receptor, mainly functions to mediate endogenous immunity and immune presentation, mediate inflammatory response and participate in the expression of inflammatory factors. It has become one of the research hotspots in tumor immunology in recent years, and plays an important role in inhibiting the regulation of tumor cell apoptosis. According to the different adaptor proteins, TLR4 can regulate tumor cell apoptosis mainly through two signaling pathways: one is MyD88-independent signaling pathway; the other is MyD88-dependent signaling pathway.<sup>(27,28)</sup> When the endogenous ligand binds to TLR4, a ligand receptor complex that aggregates MYD88 is formed, which further mediates the activation of tumor necrosis factor receptor-related factor 6 and further triggers downstream signal transduction. After activation of TRAF-6, it binds to TAK1 binding protein and subsequently activates TAK-1. Activated TAK-1 further mediates the activation of NF- $\kappa$ B, p38, and JNK signaling pathways. Our previous experiments showed that autophagy inhibitors combined with radiotherapy could effectively promote the apoptosis of ESCC, while LPS-PG could induce the activation of autophagy through TLR4/MYD88/JNK pathway, and then promote the radioresistance of ESCC. In order to further clarify the potential mechanism of LPS-PG on ESCC cells, adenovirus corresponding to TLR4, MYD88, and JNK were used for interference, and autophagy inhibitor 3-MA was added for intervention. The results suggested that LPS-PG could not only promote the autophagy activation of ESCC cells through TLR4/MYD88/JNK signaling pathway, but also promote the radioresistance of ESCC cells through TLR4/MYD88/JNK pathway. These results suggest that LPS-PG can induce autophagy activation through TLR4/MYD88/JNK pathway and promote the radioresistance of ESCC cells. As this study mainly focused on an exploratory study on the effects of PG-LPS on the proliferation, apoptosis and autophagy of acquired radiation-tolerant esophageal squamous cell cancer cells and the possible mechanism of action, parallel cell lines were not

selected for double verification. We will conduct further studies in subsequent studies. In order to further confirm the PG-LPS of radioresistance of ESCC cells role and the potential mechanism. In this study, we only used adenovirus interference for the test, without overexpression verification, which is also one of the defects of this paper.

In conclusion, LPS-PG can promote cell proliferation, inhibit cell apoptosis, promote autophagy and thus promote cell radioresistance. and its effect may be achieved by regulating the activity of TLR4/MYD88/JNK pathway.

## References

- 1 Li C, Zhu M, Lou X, *et al.* Transcriptional factor OCT4 promotes esophageal cancer metastasis by inducing epithelial-mesenchymal transition through VEGF-C/VEGFR-3 signaling pathway. *Oncotarget* 2017; **8**: 71933–71945.
- 2 Ying J, Zhang M, Qiu X, *et al.* The potential of herb medicines in the treatment of esophageal cancer. *Biomed Pharmacother* 2018; **103**: 381–390.
- 3 Chen W, Sun K, Zheng R, *et al.* Cancer incidence and mortality in China, 2014. *Chin J Cancer Res* 2018; **30**: 1–12.
- 4 Zeng H, Zheng R, Zhang S, *et al.* Esophageal cancer statistics in China, 2011: estimates based on 177 cancer registries. *Thorac Cancer* 2016; **7**: 232–237.
- 5 Jayaprakasam VS, Yeh R, Ku GY, *et al.* Role of imaging in esophageal cancer management in 2020: update for radiologists. *AJR Am J Roentgenol* 2020; **215**: 1072–1084.
- 6 Goense L, van Rossum PS, Kandioler D, *et al.* Stage-directed individualized therapy in esophageal cancer. *Ann NY Acad Sci* 2016; **1381**: 50–65.
- 7 Beckert S, Königsrainer A. Oligometastases in gastric and esophageal cancer: current clinical trials and surgical concepts. *Chirurg* 2018; **89**: 505–509. (in German)
- 8 Parzych KR, Klionsky DJ. An overview of autophagy: morphology, mechanism, and regulation. *Antioxid Redox Signal* 2014; **20**: 460–473.
- 9 Karpathiou G, Sivridis E, Koukourakis MI, *et al.* Light-chain 3A autophagic activity and prognostic significance in non-small cell lung carcinomas. *Chest* 2011; **140**: 127–134.
- 10 Digomann D, Linge A, Dubrovskaja A. SLC3A2/CD98hc, autophagy and tumor radioresistance: a link confirmed. *Autophagy* 2019; **15**: 1850–1851.
- 11 Ko A, Kanehisa A, Martins I, *et al.* Autophagy inhibition radiosensitizes *in vitro*, yet reduces radioresponses *in vivo* due to deficient immunogenic signalling. *Cell Death Differ* 2014; **21**: 92–99.
- 12 Liu M, Ma S, Liu M, *et al.* Synergistic killing of lung cancer cells by cisplatin and radiation via autophagy and apoptosis. *Oncol Lett* 2014; **7**: 1903–1910.
- 13 Lu C, Xie C. Radiation-induced autophagy promotes esophageal squamous cell carcinoma cell survival via the LKB1 pathway. *Oncol Rep* 2016; **35**: 3559–3565.
- 14 Chi L, Zhang L, Qiong F, *et al.* Autophagy inhibition enhances radiosensitivity of esophageal squamous carcinoma Eca-109 cells. *Chin J Radiol Med Prot* 2015; **35**: 165–170.
- 15 DiSiena M, Perelman A, Birk J, Rezaizadeh H. Esophageal cancer: an updated review. *South Med J* 2021; **114**: 161–168.

## Acknowledgments

The project is supported by Hubei Provincial Health Commission Joint Foundation (WJ2019H323); Foundation of Wuhan Municipal Health Commission (WX19A08).

## Conflict of Interest

No potential conflicts of interest were disclosed.

- 16 Naseri A, Salehi-Pourmehr H, Majidazar R, *et al.* Systematic review and meta-analysis of the most common genetic mutations in esophageal squamous cell carcinoma. *J Gastrointest Cancer* 2022; **53**: 1040–1049.
- 17 Reichenbach ZW, Murray MG, Saxena R, *et al.* Clinical and translational advances in esophageal squamous cell carcinoma. *Adv Cancer Res* 2019; **144**: 95–135.
- 18 Li XD, Tian W. Research progress of autophagy and tumor diseases. *World's Latest Medical Information Digest* 2020; **20**: 67–68. (in Chinese)
- 19 Ye P. Recent advances in the relationship between autophagy and tumor. *Journal of Gannan Medical College* 2018; **38**: 5. (in Chinese)
- 20 Chen N, Wu L, Yuan H, Wang J. ROS/autophagy/Nrf2 pathway mediated low-dose radiation induced radio-resistance in human lung adenocarcinoma A549 cell. *Int J Biol Sci* 2015; **11**: 833–844.
- 21 Mancias JD, Kimmelman AC. Targeting autophagy addiction in cancer. *Oncotarget* 2011; **2**: 1302–1306.
- 22 Ravanan P, Srikumar IF, Talwar P. Autophagy: the spotlight for cellular stress responses. *Life Sci* 2017; **188**: 53–67.
- 23 Adams O, Janser FA, Dislich B, *et al.* A specific expression profile of LC3B and p62 is associated with nonresponse to neoadjuvant chemotherapy in esophageal adenocarcinomas. *PLoS One* 2018; **13**: e0197610.
- 24 Wang ZB, Peng XZ, Chen SS, *et al.* High p53 and MAP1 light chain 3A co-expression predicts poor prognosis in patients with esophageal squamous cell carcinoma. *Mol Med Rep* 2013; **8**: 41–46.
- 25 Li W, Li S, Li Y, *et al.* Immunofluorescence staining protocols for major autophagy proteins including LC3, P62, and ULK1 in mammalian cells in response to normoxia and hypoxia. *Methods Mol Biol* 2019; **1854**: 175–185.
- 26 Ma JB, Hu SL, Zang RK, Su Y, Liang YC, Wang Y. MicroRNA-487a promotes proliferation of esophageal cancer cells by inhibiting p62 expression. *Eur Rev Med Pharmacol Sci* 2019; **23**: 1502–1512.
- 27 Takeda K, Akira S. TLR signaling pathways. *Semin Immunol* 2004; **16**: 3–9.
- 28 Lim KH, Staudt LM. Toll-like receptor signaling. *Cold Spring Harb Perspect Biol* 2013; **5**: a011247.



This is an open access article distributed under the terms of the Creative Commons Attribution-NonCommercial-NoDerivatives License (<http://creativecommons.org/licenses/by-nc-nd/4.0/>).